DOI: 10.1002/chem.200500724

Controlled Hydrothermal Synthesis and Structural Characterization of a Nickel Selenide Series

Zhongbin Zhuang, Qing Peng,* Jing Zhuang, Xun Wang, and Yadong Li*[a]

Abstract: A series of nickel selenides ($NiSe_2$ microcrystals, $Ni_{1-x}Se$ and Ni_3Se_2 microspheres) has been successfully synthesized through a convenient, low-temperature hydrothermal method. A good nucleation and growth environment has been created by forming a uniform and transparent solution reaction system. The compositions (including the x value of $Ni_{1-x}Se$), phase structures, as well as the morphologies of nickel selenides, can be controlled by adjusting the Ni/Se ratio of the raw materials, the pH, the reaction temperatures and times, and so forth. The newly produced Se microspheres in the system have been used as both reactant and in situ template to the $Ni_{1-x}Se$ microspheres. It is found that $Ni_{1-x}Se$ microspheres act as the intermediate precursor during the formation of Ni_3Se_2 microspheres. Under certain conditions, hexagonal NiSe microspheres can be converted into rhombohedral NiSe nanowires in solution. The formation mechanisms of a series of nickel selenides has been investigated in detail by means of X-ray diffraction (XRD) and scanning electron microscopy (SEM) analyses. This work has provided a general, simple, and effective method to control the composition, phase structure, and morphology of metal selenides in aqueous solution, which will be important for inorganic synthesis methodology and further applications of selenides.

Keywords: hydrothermal synthesis · microspheres · morphology · nickel · selenium

Introduction

Nickel selenide semiconductors exhibit interesting electronic and magnetic properties and have found several applications in the field of materials science, which has attracted considerable research attention over the last ten years or so.[1–8] Because of the valence electronic configuration of Ni ($3d^8 4s^2$) and the small difference in electronegativity between Ni ($\chi = 1.9$) and Se ($\chi = 2.4$), nickel and selenium can form a variety of nickel selenides, including non-stoichiometric compounds. According to the phase diagram,[9] at room temperature there are three stable phases: $NiSe_2$, $Ni_{1-x}Se$ (nickel content can vary from 1.00 to 0.85 relative to 1 Se), and Ni_3Se_2. The properties (including physical and chemical properties) and applications of materials are usually determined by their compositions, phase structures, and morphologies.[4,10–12] In this paper, the controlled synthesis of a series of nickel selenides ($NiSe_2$, $Ni_{1-x}Se$ ($x = 0$–0.15), and Ni_3Se_2) has been investigated in aqueous solution, and a simple, convenient, and effective controlled synthetic procedure has been developed.

Traditionally, nickel selenides were synthesized by using a variety of methods, such as solid-state synthesis,[13] molecular precursors,[14] elemental direct reactions,[15] ultrasonic synthesis,[16] and mechanical alloying (MA).[17] However, these methods often need a high temperature or use toxic metallorganic reagents as precursors and usually need a special device. Few of these methods can be used to controllably and systematically synthesize a series of nickel selenides. The solvothermal synthetic method has also been developed by using organic solvents, such as pyridine or ethylenediamine, at around 180 °C.[18] However, it is still a challenge to obtain a series of nickel selenides ($NiSe_2$, $Ni_{1-x}Se$, and Ni_3Se_2) and systematically control their compositions, phase structures, and morphologies in aqueous solution.

Recently, Na_2SeO_3 was selected in our experiments to provide a highly reactive selenium source in aqueous solution and has given good results.[19] Following this method, we herein report a convenient and controllable synthetic

---

[a] Z. Zhuang, Dr. Q. Peng, J. Zhuang, Dr. X. Wang, Prof. Y. Li
Department of Chemistry and the Key Laboratory of Atomic and Molecular Nanosciences (National Center for Nanoscience and Nanotechnology Ministry of Education, China)
Tsinghua University, Beijing, 100084 (P.R. China)
Fax: (+86) 10-6278-8765
E-mail: pengqing@mail.tsinghua.edu.cn
ydli@mail.tsinghua.edu.cn

Supporting information for this article is available on the WWW under http://www.chemeurj.org/ or from the author.

method for obtaining a series of nickel selenides. By simply adjusting the molar ratio of the reactants, the temperature, the pH, or the reaction times, all of the three stable phases found at room temperature (hexagonal $Ni_{1-x}Se$, rhombohedral Ni_3Se_2, and cubic $NiSe_2$) can be obtained, and their compositions, structural phases, and morphologies can be easily controlled.

Experimental Section

Materials: All the reagents were of analytical grade and were used as received without any further purification. Deionized water was used throughout. Nickel sulfate ($NiSO_4{\cdot}7H_2O$), sodium selenite ($Na_2SeO_3{\cdot}5H_2O$), ethylenediaminetetraacetic acid (EDTA), sodium hydroxide (NaOH), and hydrazine hydrate ($N_2H_4{\cdot}H_2O$, 80%) were purchased from the Beijing Chemical Factory, China.

Synthesis of $NiSe_2$, $Ni_{1-x}Se$, and Ni_3Se_2: In a typical synthesis of $Ni_{1-x}Se$ (including NiSe), the original molar ratio between $NiSO_4{\cdot}7H_2O$ and $Na_2SeO_3{\cdot}5H_2O$ was selected to be 1:3. $NiSO_4{\cdot}7H_2O$ (0.28 g, 0.001 M) was put into a Teflon-lined autoclave of 50 mL capacity and dissolved in deionized water (30 mL). The chelating agent, EDTA (1.0 g, ≈0.003 M), was added to the solution. NaOH (1.0 g, 0.025 M) was added later to keep the pH value at about 14. After mixing for 5 min under stirring, $Na_2SeO_3{\cdot}5H_2O$ (0.78 g, 0.003 M) was added to the mixture. Lastly, hydrazine hydrate (10 mL) was added to the mixture and the system finally formed a transparent solution. After stirring for 5 min, the autoclave was sealed and heated for 5 h. Then, the autoclave was allowed to cool to room temperature naturally. The product was obtained and collected by filtration, washed with deionized water and absolute ethanol, and then dried at 60 °C. For $Ni_{0.85}Se$, the reaction temperature was set at 100 °C, and for NiSe, the reaction temperature was elevated to 180 °C. $Ni_{1-x}Se$ ($x=0$–0.15) was obtained by controlling the reaction temperature between 100 and 180 °C.

Similarly, Ni_3Se_2 was prepared by changing the molar ratio between $NiSO_4{\cdot}7H_2O$ and $Na_2SeO_3{\cdot}5H_2O$ to 3:1, so the amounts of $NiSO_4{\cdot}7H_2O$ and $Na_2SeO_3{\cdot}5H_2O$ introduced were 0.84 and 0.26 g, respectively. The reaction time was 7 h and the reaction temperature was 180 °C.

For $NiSe_2$, just like the synthesis of $Ni_{1-x}Se$, the molar ratio of $NiSO_4{\cdot}7H_2O$ and $Na_2SeO_3{\cdot}5H_2O$ was selected to be 1:3, but the pH value was adjusted from 14 to 10. The reaction time was 20 h and the reaction temperature was 140 °C. After the reaction, the product was added to hydrazine hydrate (50 mL) to dissolve the excess unreacted Se, and then collected, washed, and dried at 60 °C.

Characterization: The phase purity of the products was examined by using X-ray diffraction (XRD) on a Bruker D8 Advance X-ray powder diffractometer with $Cu_{K\alpha}$ radiation ($\lambda=1.5418$ Å). The operation voltage and current were kept at 40 kV and 40 mA, respectively. A 2θ range from 10 to 70° was covered in steps of 0.02° with a count time of 0.2 s. The sample size, morphology, and elemental composition of the products were examined by means of scanning electron microscopy (SEM) and energy-dispersive X-ray spectroscopy (EDX) analyses by using a JEOL JSM-6301F scanning electron microscope operating at 20 kV.

Results and Discussion

Crystal structures of $NiSe_2$, $Ni_{1-x}Se$, and Ni_3Se_2: In our homogeneous-solution reaction system, a good environment for the nucleation and growth of the product is provided. The morphologies and structures of as-prepared nickel selenides can be determined by their crystal structures to a certain extent. Figure 1 shows schematic illustrations of the often observed crystal structures of $NiSe_2$, $Ni_{1-x}Se$, and Ni_3Se_2. $NiSe_2$ has a cubic pyrite structure (Figure 1a), which has dumbbell-shaped Se_2 units between two Ni atoms. It usually forms an isotropic structure after the reaction. $Ni_{1-x}Se$ ($x=0$–0.15, Figure 1b) usually exists in an anisotropic hexagonal nickel arsenide structure. Due to its unique *c* axis, the growth rate of $Ni_{1-x}Se$ along the *a*, *b*, and *c* axes is usually different and $Ni_{1-x}Se$ often shows anisotropic morphology. $Ni_{1-x}Se$ can also crystallize in its thermodynamically stable phase, that is, as a rhombohedral structure (not shown). Compared with the nickel arsenide structure, the rhombohedral structure shows more anisotropism. For Ni_3Se_2, the rhombohedral structure (Figure 1c) is the often observed phase after the reaction.

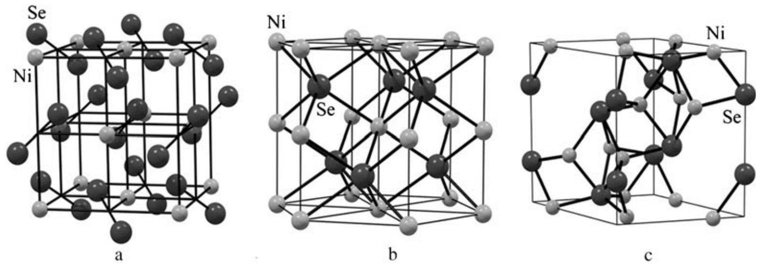

Figure 1. Schematic illustrations of the commonly observed crystal structures of a) $NiSe_2$, b) $Ni_{1-x}Se$, and c) Ni_3Se_2.

XRD studies: It was found that the original molar ratios of the reactants (Ni/Se), the reaction temperature, and the pH played important roles in the formation of the nickel selenide series in our aqueous reaction system. Table 1 lists the reaction conditions and the yields for the synthesis of $NiSe_2$, $Ni_{1-x}Se$, and Ni_3Se_2. The yields are calculated with respect to $NiSO_4{\cdot}7H_2O$ (for $NiSe_2$ and $Ni_{1-x}Se$) or $Na_2SeO_3{\cdot}5H_2O$ (for Ni_3Se_2).

Table 1. The reaction conditions of nickel selenides synthesized from $NiSO_4{\cdot}7H_2O$ and $Na_2SeO_3{\cdot}5H_2O$.

T [°C]	Ni/Se ratio (reactants)	pH	*t* [h]	Product	Yield [%]
100–180	1:3	14	5	$Ni_{1-x}Se$	≈95
140	1:3	10	20	$NiSe_2$	≈82
180	3:1	14	7	Ni_3Se_2	≈92

Figure 2 shows the XRD patterns of as-prepared $NiSe_2$, $Ni_{1-x}Se$, and Ni_3Se_2, which indicate that all these samples are pure-phase compounds. Due to the excess of chelating agent (EDTA) in the reaction system, no other peaks of nickel impurities (such as nickel hydroxide) are observed. The results are in good agreement with those reported in

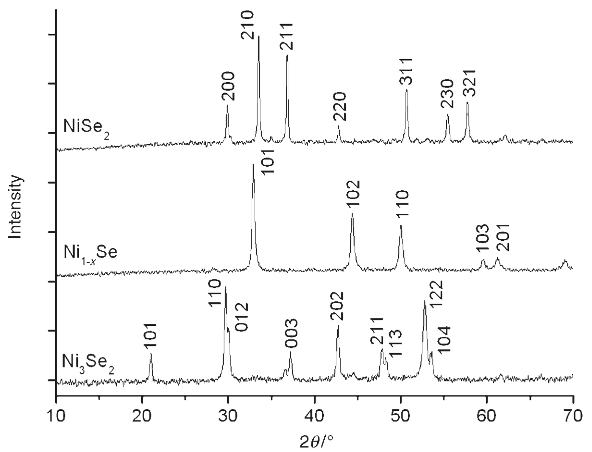

Figure 2. XRD patterns of cubic $NiSe_2$, hexagonal $Ni_{1-x}Se$, and rhombohedral Ni_3Se_2.

the literature ($NiSe_2$: JCPDS card number 41-1495; $Ni_{1-x}Se$: JCPDS card number 18-888; Ni_3Se_2: JCPDS card number 19-841). The peaks are strong and narrow, which indicates the good crystallinity of the as-prepared samples.

During the synthesis of $Ni_{1-x}Se$, by adjusting the reaction temperature from 100 to 180 °C, the x value can be varied from 0.15 to 0. In our experiments, it was found that excess $NiSO_4 \cdot 7H_2O$ and high reaction temperature favor the formation of compounds with high nickel content. Figure 3 shows the XRD patterns of two extreme conditions (NiSe obtained at 180 °C and $Ni_{0.85}Se$ obtained at 100 °C) and an intermediate state ($Ni_{1-x}Se$ ($0<x<0.15$) obtained at 140 °C). As the nickel content increases, all the peaks (101, 102, and 110, etc.) in the XRD pattern are found to have a tiny shift to a smaller value of 2θ (corresponding to an increase in d, the interplanar spacing between the atoms in the crystal), which indicates that the volume of the crystal unit cell of $Ni_{1-x}Se$ is also increasing.

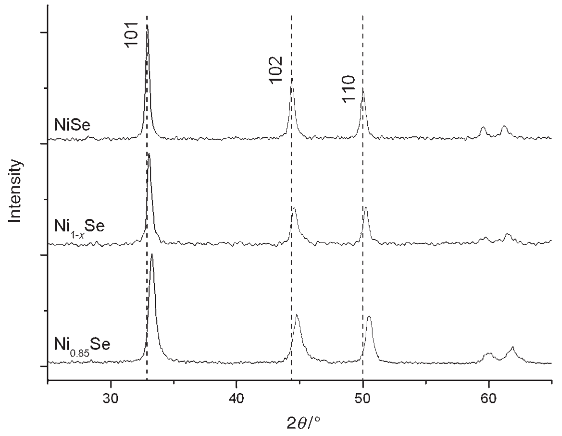

Figure 3. XRD patterns of NiSe (180 °C), $Ni_{1-x}Se$ (140 °C), and $Ni_{0.85}Se$ (100 °C).

At low reaction temperatures (ca. 100–120 °C, pH 14) and with relatively short reaction times (about 4 h), although the original molar ratio of Ni/Se is 3:1 or 1:3, $Ni_{1-x}Se$ is obtained instead of Ni_3Se_2 or $NiSe_2$. The x value is also found to vary from 0 to 0.15 when the ratio of Ni/Se is changed from 3:1 to 1:1 and to 1:3.

In the synthesis of $NiSe_2$, the ideal reaction temperature and pH value are 140 °C and 10, respectively. When the reaction temperature is elevated to 180 °C, NiSe emerges and a mixture of $NiSe_2$ and NiSe is obtained. When the pH value is 14, pure-phase NiSe is the final product instead of $NiSe_2$.

Long reaction times lead to a preference for the formation of a thermodynamically stable phase. In the synthesis of NiSe at 180 °C, when the starting molar ratio of Ni/Se is adjusted to 1:1, hexagonal NiSe will be obtained first after a short reaction time. With the extension of reaction time, hexagonal NiSe will gradually transform into rhombohedral NiSe. Figure 4 shows the evolution of XRD patterns from hexagonal to rhombohedral NiSe. When the reaction time is four hours, the product is pure hexagonal NiSe. The characteristic peaks of rhombohedral NiSe appear after 20 hours. When the reaction time is lengthened to 65 hours, the main product is rhombohedral NiSe. However, with an even longer reaction time, a small amount of hexagonal NiSe still exists in the product. The ratio of hexagonal to rhombohedral NiSe appears to remain unchanged after a long reaction time. It is worth noting that this phase-conversion phenomenon cannot be observed in reaction systems with excess selenium (such as Ni/Se = 1:3).

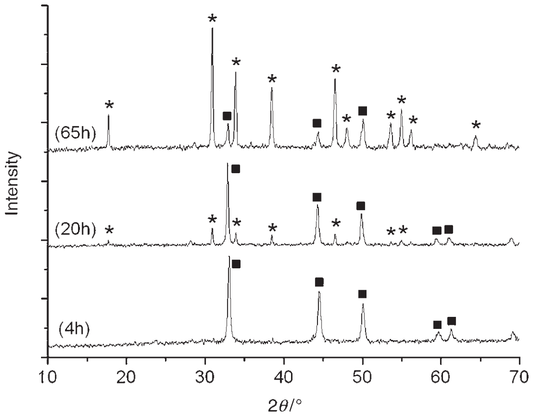

Figure 4. Evolution of the XRD patterns with reaction times from hexagonal NiSe (■) to rhombohedral NiSe (*).

Morphologies of the samples: Scanning electron microscopy (SEM) was employed to investigate the morphologies of the as-prepared nickel selenide series. In our experiments, $Ni_{1-x}Se$ samples obtained from reactions at 100 to 180 °C are all microspheres. Figures 5a and b show the SEM images of $Ni_{1-x}Se$ obtained at 140 °C. These microspheres are not very uniform and have an average diameter of about 1 μm. From

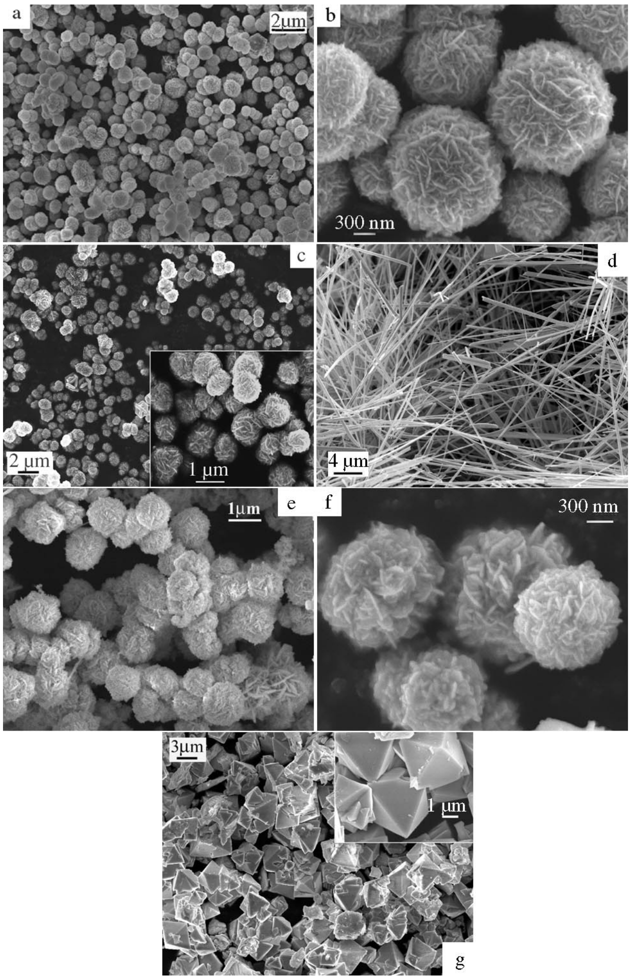

Figure 5. SEM images of the nickel selenide series: a, b) $Ni_{1-x}Se$ microspheres obtained at 140 °C; c) hexagonal NiSe microspheres obtained at 180 °C; d) rhombohedral NiSe nanowires obtained at 180 °C (65 h); e, f) Ni_3Se_2 microspheres obtained at 180 °C; g) octahedral-shaped $NiSe_2$ microcrystals (140 °C, pH 10).

the magnified SEM image (Figure 5b), it can be observed that the surface of the $Ni_{1-x}Se$ microspheres is not smooth. It is built up of many nanoplates, which makes the spheres look very rugged. These nanoplates constitute many active positions on the surface and make the microspheres have a larger surface area than that of smooth microspheres, which make this type of microsphere have potential for applications such as catalysis, field emission, and gas sensors. Figure 5c shows the NiSe microspheres obtained at 180 °C. Compared with $Ni_{1-x}Se$ obtained at 140 °C, these microspheres have a smaller average diameter. This can be explained by considering that at a relatively high temperature, more NiSe nuclei will form before the growth process, which will cause the formation of more spheres with smaller diameters. Figure 5d shows the image of rhombohedral NiSe obtained at 180 °C (Ni/Se = 1:1) after a reaction time of 65 hours. It is interesting to note that nanowires are obtained instead of microspheres, with lengths of about 30 μm and diameters of about 200 nm. Ni_3Se_2 (Figures 5e and f, obtained at 180 °C) also have microspherical morphology. From the magnified SEM image (Figure 5f), it can be observed that they have a similar surface and diameter to that of $Ni_{1-x}Se$ microspheres. Figure 5g shows the morphology of $NiSe_2$. Due to its cubic pyrite structure, octahedral-shaped microcrystals are obtained in our homogeneous-solution reaction system. From the magnified SEM image inset in Figure 5g, it can be found that the average length of the edge of these microcrystals is about 3–4 μm.

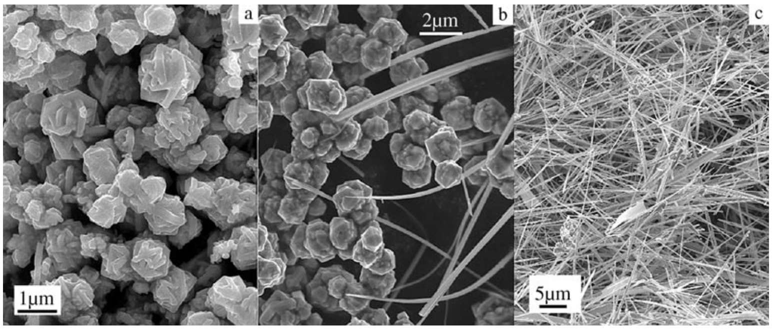

Figure 6. SEM images showing the conversion process from hexagonal to rhombohedral NiSe: a) irregular-polyhedron-shaped hexagonal NiSe at 4 h; b) hexagonal NiSe polyhedrons and rhombohedral NiSe nanowires at 20 h; c) rhombohedral NiSe nanowires at 65 h.

To investigate the conversion process from hexagonal to rhombohedral NiSe occurring at 180 °C when the original molar ratio of Ni/Se was adjusted to 1:1, SEM analysis (Figure 6) was used to characterize the samples at different conversion steps. In agreement with the XRD patterns (Figure 4), unlike the sphere-shaped $Ni_{1-x}Se$ obtained from a Ni/Se ratio of 1:3, the hexagonal sample (Figure 6a) formed after 4 hours shows irregular polyhedral morphology. When the reaction time was 20 hours, it was found that the rhombohedral NiSe nanowires appear (Figure 6b), which is consistent with the XRD results. When the reaction time was lengthened to 65 hours, almost all the products had been converted into nanowires (Figure 6c); the XRD results also led to this conclusion. From the EDX results (see the Supporting Information), it was found that both the polyhedrons and nanowires are pure nickel selenide with a Ni/Se ratio of about 1:1.

Formation of $Ni_{1-x}Se$ microspheres and $NiSe_2$ microcrystals: In our experiments, the Ni/Se ratio of the raw materials, the chelating agent (EDTA), the pH, and the reaction time were used to control the formation, nucleation, and growth of nickel selenides. For the formation of nickel selenides, Ni^{2+} coordinates with EDTA first and forms a stable chelate complex. The concentration of free Ni^{2+} in the solution is very low, which can prevent the deposition of $NiSeO_3$

before the formation of selenides. The uniformity of the reaction solution provides a good environment for growing high quality nickel selenide nanocrystals. The water soluble Na_2SeO_3 was used as the Se source. Under alkaline conditions, SeO_3^{2-} can be quickly reduced to elemental Se upon heating ($SeO_3^{2-}+3H_2O+4e^- \rightarrow Se+6OH^-$),[19,20] and the newly produced Se will be further converted to Se^{2-} through a disproportionation process ($3Se+6OH^- \rightarrow 2Se^{2-}+SeO_3^{2-}+3H_2O$). It is clear that the disproportionation of Se is dependent on the alkalinity of the solution. The stronger the alkalinity, the more completely Se converts to Se^{2-}.

By controlling the pH of the reaction solution, it can be very easy to control the formation of metal monoselenide or diselenide. When the pH value is set to 14, almost all the elemental Se will be converted to Se^{2-} and $Ni_{1-x}Se$ will be formed ($(1-x)Ni^{2+}+(1-x)Se^{2-}+x\,Se \rightarrow Ni_{1-x}Se$). When the pH value is adjusted to 10, only a part of the Se present can be converted, so there is still some elemental Se existing in the system. Se will combine with Se^{2-} to form Se_2^{2-}, and $NiSe_2$ will be the final product ($Ni^{2+}+Se^{2-}+Se \rightarrow NiSe_2$). Due to its cubic crystal structure, the $NiSe_2$ obtained in our homogeneous-solution reaction system shows octahedral morphology.

Unlike other metal ions (e.g., Zn^{2+}, Cd^{2+}), Ni^{2+} in aqueous solution can be reduced by hydrazine to elemental Ni upon heating.[21] Therefore, another possible route is that the newly produced Se and Ni will react with each other and produce $Ni_{1-x}Se$ (pH 14) and $NiSe_2$ (pH 10) directly. Based on earlier studies of the formation of ZnSe and CdSe,[19] the disproportionation process is considered to be the main process in the reaction.

As reported in the literature,[20] the newly produced elemental Se has an amorphous structure in alkaline solution and often aggregates to form a spherical morphology. This may be the reason that the $Ni_{1-x}Se$ obtained in the experiments also has a spherical structure. Figure 7 shows the schematic representation of the formation mechanism of $Ni_{1-x}Se$ microspheres. In our reaction system with excess Se (Ni/Se = 1:3), the intermediate compound (amorphous Se microspheres) produced in the reaction is the template for the formation of $Ni_{1-x}Se$. Around the Se microspheres, there is a relatively high concentration of Se^{2-} (from the disproportionation of the outer layer of the Se microspheres), and $Ni_{1-x}Se$ nanocrystals precipitate on the surface of the Se microspheres until all of the Ni^{2+} is consumed (step a). Under strong alkaline conditions, the unreacted excess Se inside the spheres is gradually converted to Se^{2-} and SeO_3^{2-} and dissolves in the solution through disproportionation (step b). During step b, as well as the ageing stage after Se dissolves, $Ni_{1-x}Se$ nanocrystals aggregate to form a solid spherical structure (step c). Due to the anisotropic crystal structure, based on the precipitation solubility equilibrium in the solution, $Ni_{1-x}Se$ located on the outer layer of the microspheres gradually dissolves and crystallizes along certain orientations to form nanoplates on the surface of the spheres. When the original molar ratio of Ni/Se is adjusted to 1:1, in the reaction all Se microsphere are consumed to form $Ni_{1-x}Se$ (no excess Se exists inside to provide a supporter), and finally irregular polyhedral morphology is obtained.

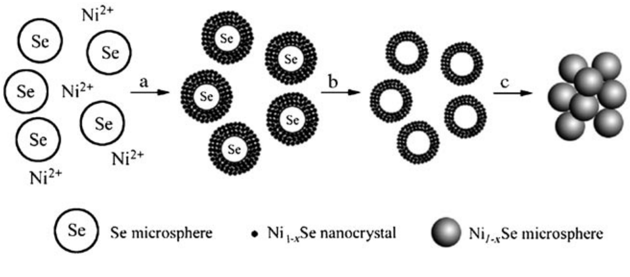

Figure 7. Schematic representation of the formation mechanism of $Ni_{1-x}Se$ microspheres.

Formation of Ni_3Se_2 microspheres and the conversion from $Ni_{1-x}Se$ to Ni_3Se_2: In our experiments, pure-phase Ni_3Se_2 can be obtained in the reaction system with excess nickel. It is found that $Ni_{1-x}Se$ is the intermediate compound during the formation of Ni_3Se_2. In order to investigate the conversion process from $Ni_{1-x}Se$ to Ni_3Se_2, the product was taken out after reaction for three, five, and seven hours and characterized by XRD analysis. Figure 8 shows the evolution of the XRD patterns. First, pure-phase $Ni_{1-x}Se$ (marked with ■) was obtained when the reaction time was three hours. With a longer reaction time, the characteristic peaks of Ni_3Se_2 (marked with *) appeared at five hours. After seven hours, only Ni_3Se_2 peaks could be observed, which indicates that all the $Ni_{1-x}Se$ had been consumed and that a pure-phase Ni_3Se_2 had been produced. Based on the experiment, it was realized that the conversion process from $Ni_{1-x}Se$ to Ni_3Se_2 is very fast.

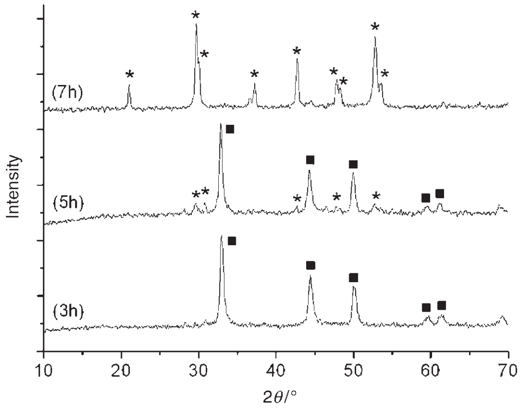

Figure 8. Evolution of the XRD patterns from $Ni_{1-x}Se$ (■) to Ni_3Se_2 (*) with different reaction times at 180 °C (Ni/Se = 3:1, pH 14).

For the formation mechanism of Ni_3Se_2, it can be considered that, in the reaction system with excess nickel, Ni^{2+} will react with Se^{2-} and produce $Ni_{1-x}Se$ first until all the Se source is used up. With the presence of hydrazine hydrate, the excess Ni^{2+} will be reduced to elemental Ni upon heating.[21] This kind of newly produced Ni is highly reactive and will react with $Ni_{1-x}Se$ to produce Ni_3Se_2 through Equations (1) and (2):

$$2\,Ni^{2+} + N_2H_4 + 4\,OH^- \rightarrow 2\,Ni + N_2 + 4\,H_2O \tag{1}$$

$$2\,Ni_{1-x}Se + (1+2x)Ni \rightarrow Ni_3Se_2 \tag{2}$$

In the XRD patterns, no characteristic peaks of elemental Ni is found, and this can be attributed to the strong chelation properties of EDTA, which caused the low concentration of free Ni^{2+} during the reaction. The amount of elemental Ni is very small and thus the characteristic peaks cannot be observed from XRD analysis.

In this conversion, the intermediate compound ($Ni_{1-x}Se$) acts as both the reactant and the template in the formation of Ni_3Se_2. Therefore, the morphology of Ni_3Se_2 is certainly determined by the morphology of $Ni_{1-x}Se$. This is the reason that Ni_3Se_2 also has a spherical structure, and the surface is not smooth but instead built up of many nanoplates, similar to that of $Ni_{1-x}Se$.

Conversion mechanism from hexagonal to rhombohedral NiSe with long reaction times: In our experiments, it was found that the formation of hexagonal and rhombohedral NiSe is a competitive process between kinetic and thermodynamic control. At the beginning of the reaction, the concentration of the NiSe monomer (single NiSe molecule before its nucleation and growth) becomes higher and higher, which causes a high crystallization and growth rate of NiSe. At this time, hexagonal NiSe is produced and the kinetic control is the main factor. When all the Se and Ni sources are consumed, the precipitation–solubility equilibrium of NiSe in solution becomes the main reaction. At this time, thermodynamic control is the main factor and hexagonal NiSe will gradually convert to the thermodynamically stable rhombohedral NiSe. Compared with the hexagonal structure, the rhombohedral structure has a stronger anisotropy, which is the reason why the product morphology changes from microspheres to nanowires accompanied with the phase conversion. This experiment has proved from another point of view that crystal structure plays an important role in the formation of nanostructures. Phase conversion (from isotropic to anisotropy, from small to large anisotropy, etc.) can be used in the controlled synthesis of different nanostructures.

The above conversion can only be observed when the original molar ratio of Ni/Se is 1:1. Under the condition of Ni/Se = 1:3 (reaction system with excess selenium), the hexagonal product remains unchanged in the experiments after reacting for 65 hours. The reason for this is that the phase-conversion process is based on the precipitation–solubility equilibrium of NiSe. In the reaction system with excess selenium, the concentration of Se^{2-} in the solution is relatively high, which makes the solubility equilibrium shift to the NiSe direction. Under this condition, NiSe has an extra small solubility, and this makes it difficult for it to convert to the rhombohedral product.

Conclusion

In summary, by controlling the Ni/Se ratio of the raw materials, the pH, and the reaction time, a nickel selenide series ($NiSe_2$, $Ni_{1-x}Se$, Ni_3Se_2) can be selectively synthesized in aqueous solution through a convenient, low-temperature hydrothermal method. The x value of $Ni_{1-x}Se$ can be adjusted from 0–0.15. In the reaction system with excess selenium, amorphous Se microspheres produced in the reaction can be used as both the reactant and the template. On the basis of this, $Ni_{1-x}Se$ microspheres and $NiSe_2$ microcrystals are obtained. Ni_3Se_2 microspheres can be produced in reaction systems with excess nickel, and are found to come from $Ni_{1-x}Se$ microspheres during the reaction. When the Ni/Se ratio of the raw materials is 1:1, the hexagonal NiSe microspheres can be converted to rhombohedral NiSe nanowires in solution upon heating with long reaction times. The formation and conversion mechanism of nickel selenides has been investigated in detail. This work is valuable for the understanding of the formation of metal selenides in aqueous solution. It has provided a general, simple, and effective method to control the compositions, phase structures, and morphologies of metal selenides, which will be very important for inorganic synthesis methodology and further applications of selenides.

Acknowledgements

This work was supported by the National Natural Science Foundation of China (NSFC; 20401010, 90406003, 50372030, 20025102, 20131030), the Foundation for the Author of National Excellent Doctoral Dissertation of P.R. China, and the State Key Project of Fundamental Research for Nanomaterials and Nanostructures (2003CB716901).

---

[1] W. S. Sheldrick, M. Wachhold, *Angew. Chem.* **1997**, *109*, 214; *Angew. Chem. Int. Ed. Engl.* **1997**, *36*, 206.
[2] G. Parkin, *Prog. Inorg. Chem.* **1998**, *47*, 1.
[3] a) M. L. Steigerwald, L. E. Brus, *Acc. Chem. Res.* **1990**, *23*, 183; b) Y. Wang, N. Herron, *J. Phys. Chem.* **1991**, *95*, 525.
[4] a) A. P. Alivisatos, *Science* **1996**, *271*, 933; b) J. M. Honig, J. Spalek, *Chem. Mater.* **1998**, *10*, 2910; c) A. Y. Matsuura, H. Watanabe, C. Kim, S. Doniach, Z. X. Shen, *Phys. Rev. B* **1998**, *58*, 3690.
[5] a) X. G. Peng, L. Manna, W. D. Yang, J. Wickham, E. Scher, A. Kadavanich, A. P. Alivisatos, *Nature* **2000**, *404*, 59; b) J. T. Hu, L. S. Li, W. D. Yang, L. Manna, L. W. Wang, A. P. Alivisatos, *Science* **2001**, *292*, 2060; c) F. V. Mikulec, M. Kuno, M. Bennati, D. A. Hall, R. G. Griffin, M. G. Bawendi, *J. Am. Chem. Soc.* **2000**, *122*, 2532.
[6] a) W. H. Xie, Y. Q. Xu, B. G. Liu, D. G. Pettifor, *Phys. Rev. Lett.* **2003**, *91*, 037204; b) A. Chakrabarti, *Phys. Rev. B* **2000**, *62*, 1806; c) P. Gütlich, K. J. Range, C. Felser, C. Schultz-Munzenberg, W. Tremel, D. Walcher, M. Waldeck, *Angew. Chem.* **1999**, *111*, 2524; *Angew. Chem. Int. Ed.* **1999**, *38*, 2381; d) T. Miyazaki, H. Fujimoto, K. Ichimura, K. P. Lee, S. Hasegawa, H. Inokuchi, *Chem. Phys.* **1995**, *201*, 539.
[7] a) P. D. Fan, P. Deglmann, R. Ahlrich, *Chem. Eur. J.* **2002**, *8*, 1059; b) X. Ribas, J. C. Dias, J. Morgado, K. Wurst, E. Molins, E. Ruiz, M.

Aleida, J. Veciana, C. Rovira, *Chem. Eur. J.* **2004**, *10*, 1691; c) M. A. Petrukhina, C. Henck, B. Li, E. Block, J. Jin, S. Z. Zhang, R. Clerac, *Inorg. Chem.* **2005**, *44*, 77.

[8] a) C. E. M. Campos, J. C. de Lima, T. A. Grandi, K. D. Machado, J. P. Itie, A. Polian, *J. Solid State Chem.* **2005**, *178*, 93; b) V. L. Miller, W. L. Lee, G. Lawes, N. P. Ong, R. J. Cava, *J. Solid State Chem.* **2005**, *178*, 1508; c) S. T. Lakshmikvmar, *Sol. Energy Mater. Sol. Cells* **1994**, *32*, 7; d) M. A. Haase, J. Qiu, J. M. Depuydt, H. Cheng, *Appl. Phys. Lett.* **1991**, *59*, 1272.

[9] H. Baker, *ASM Handbook, Vol. 3*: *Phase Diagrams*, ASM International, New York, **1992**, pp. 2–317.

[10] a) M. A. El-Sayed, *Acc. Chem. Res.* **2004**, *37*, 326; b) M. A. El-Sayed, *Acc. Chem. Res.* **2001**, *34*, 257; c) J. Z. Zhang, *Acc. Chem. Res.* **1997**, *30*, 423.

[11] a) R. P. Cowburn, *J. Phys. D* **2000**, *33*, R1; b) Y. Xia, B. Gates, Y. Yin, Y Lu, *Adv. Mater.* **2000**, *12*, 693; c) Y. Xia, P. Yang, Y. Sun, Y. Wu, B. Mayers, B. Gates, Y. Yin, F. Kim, H. Yan, *Adv. Mater.* **2003**, *15*, 353.

[12] a) B. O. Dabbousi, J. Rodrigo-Viejo, F. V. Mikulec, J. R. Heine, H. Mattousi, R. Ober, K. F. Jensen, M. G. Bawendi, *J. Phys. Chem. A* **1997**, *101*, 9463; b) L. S. Li, N. Pradhan, Y. J. Wang, X. G. Peng, *Nano Lett.* **2004**, *4*, 2261.

[13] a) P. R. Bonneau, R. F. Jarvis; R. B. Kaner, *Nature* **1991**, *349*, 510; b) I. P. Parkin, *Chem. Soc. Rev.* **1996**, *25*, 199; c) G. A. Shaw, D. E. Morrison, I. P. Parkin, *J. Chem. Soc. Dalton Trans.* **2001**, 1872.

[14] a) J. G. Brennan, T. Siegrist, Y. U. Kwon, S. M. Stuczynski, M. L. Steigerwald, *J. Am. Chem. Soc.* **1992**, *114*, 10334; b) X. J. Song, M. Bochmann, *J. Chem. Soc. Dalton Trans.* **1997**, 2689.

[15] G. Henshaw, I. P. Parkin, G. A. Shaw, *J. Chem. Soc. Dalton Trans.* **1997**, 231.

[16] J. P. Ge, Y. D. Li, *J. Mater. Chem.* **2003**, *13*, 911.

[17] a) C. E. M. Campos, J. C. de Lima, T. A. Grandi, K. D. Machado, P. S. Pizani, R. Hinrichs, *Solid State Commun.* **2003**, *128*, 229; b) C. E. M. Campos, J. C. de Lima, T. A. Grandi, K. D. Machado, P. S. Pizani, R. Hinrichs, *Solid State Ionics* **2004**, *168*, 205; c) T. Ohtani, K. Maruyama, K. Ohshima, *Mater. Res. Bull.* **1997**, *32*, 343.

[18] a) Y. D. Li, Z. Y. Wang, Y. Ding, *Inorg. Chem.* **1999**, *38*, 4737; b) R. Kerner, O. Palchik, A. Gedanken, *Chem. Mater.* **2001**, *13*, 1413; c) Z. H. Han, S. H. Yu, Y. P. Li, H. Q. Zhao, F. Q. Li, Y. Xie, Q. T. Qian, *Chem. Mater.* **1999**, *11*, 2302; d) J. Yang, G. H. Cheng, J. H. Zeng, S. H. Yu, X. M. Liu, Y. T. Qian, *Chem. Mater.* **2001**, *13*, 848.

[19] a) Q. Peng, Y. J. Dong, Z. X. Deng, Y. D. Li, *Inorg. Chem.* **2002**, *41*, 5249; b) Q. Peng, Y. J. Dong, Z. X. Deng, H. Z. Kou, S. Gao, Y. D. Li, *J. Phys. Chem. B* **2002**, *106*, 9261; c) Q. Peng, Y. J. Dong, Y. D. Li, *Angew. Chem.* **2003**, *115*, 3135–3138; *Angew. Chem. Int. Ed.* **2003**, *42*, 3027–3030.

[20] a) B. Gates, B. Mayers, A. Grossman, Y. N. Xia, *Adv. Mater.* **2002**, *14*, 1749; b) U. Jeong, Y. N. Xia, *Adv. Mater.* **2005**, *17*, 102.

[21] Y. D. Li, L. Q. Li, H. W. Liao, H. R. Wang, *J. Mater. Chem.* **1999**, *9*, 2675.

Received: June 24, 2005